

Li, Z., Marsh, J. H. and Hou, L. (2020) High Precision Laser Ranging Based on STM32 Microcontroller. In: 5th International Conference on the UK-China Emerging Technologies (UCET 2020), Glasgow, UK, 20-21 Aug 2020, ISBN 9781728194882 (doi:[10.1109/UCET51115.2020.9205377](https://doi.org/10.1109/UCET51115.2020.9205377)).

This is the author's final accepted version.

There may be differences between this version and the published version. You are advised to consult the publisher's version if you wish to cite from it.

<http://eprints.gla.ac.uk/221816/>

Deposited on: 06 August 2020

High Precision Laser Ranging Based on STM32 Microcontroller

Zongkang Li
Glasgow College
University of Electronic Science and
Technology of China
Chengdu, China
2288875L@student.gla.ac.uk

John H. Marsh
James Watt School of Engineering
University of Glasgow
Glasgow, G12 8QQ, UK
John.Marsh@glasgow.ac.uk

Lianping Hou
James Watt School of Engineering
University of Glasgow
Glasgow, G12 8QQ, UK
Lianping.Hou@glasgow.ac.uk

Abstract—A miniature portable laser ranging system based on an STM32 microcontroller and VL53L0X time-of-flight laser ranging sensor was developed. An LCD display indicates the real time measured range value. Two working modes with different accuracy and detectable range were designed. These comprise high accuracy and long-distance modes which make the equipment very versatile for real applications. Following code optimization and verification by calipers, the relative measurement error is around 1% - 2% for both modes.

Keywords—laser ranging, STM32, two modes

I. INTRODUCTION

In both industrial and research areas of electronic engineering, distance information is regarded as one of the critical measurements [1]. In order to obtain accurate and reliable distance data, equipment with range detection ability is now widely used in military and industry, including infrared (IR) and ultrasonic range finders. However, many problems with accuracy arise using these traditional range systems as they are very sensitive to their surroundings, especially when exposed to unstructured and unpredictable physical environments (dust, temperature, smoke) or environments with confusing structure (rubble, debris, etc.) [2]. A more reliable method of range detection is therefore proposed. The laser diode emits a highly directional beam, and has the advantages of small size, high brightness, pure color, high energy density and high efficiency [3][4]. Most importantly, laser ranging systems are less vulnerable to environmental influences because the distance and direction of a target can be obtained by measuring the time interval, frequency variation and beam direction of the reflection and scattered echo signal. The measurement error using the laser ranging method is only one-fifth to one-hundredth of that of other optical range finders [5]. At first, phase laser ranging method gains great popularity because of its high accuracy. However, its application problems cannot be ignored. It is observed that near-zero step error could happen possibly as a result of phase-folding or phase-blurring under the influences of frequency drift, noise and atmospheric refraction [6]. Barreto et al. applied triangulation laser ranging method but its sensitivity requirement is stringent and power consumption is high [7]. In this paper, a miniature, and portable and low power consumption laser ranging system has been developed with two modes of measurement: a high accuracy mode and a long-distance mode. In this paper, a miniature and portable laser ranging system has been developed with two modes of measurement: a high accuracy mode and a long-distance mode. The system is based on the VL53L0X time-of-flight laser ranging sensor and STM32F407 microcontroller [8].

II. LASER RANGING BASED ON STM32

A. Basic principle

The VL53L0X, in which a 940 nm vertical-cavity surface-emitting laser (VCSEL) is used as the source, was selected as the laser ranging module for the system reported in this paper. During pulsed laser ranging measurements, the repetition frequency can reach a maximum of 4 kHz. Fig. 1 shows a schematic diagram of a pulsed laser ranging system.

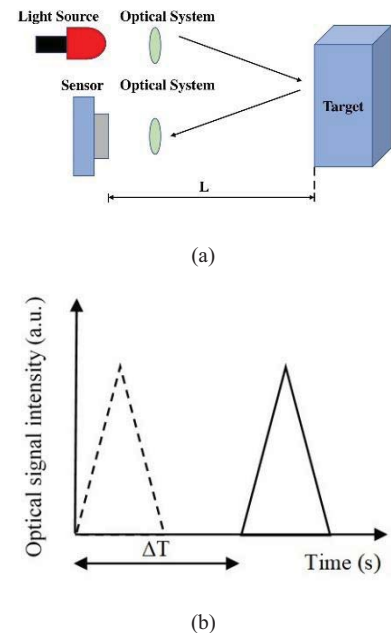


Fig. 1. Schematic diagram of the pulsed laser ranging system.

Generally, distance is measured by detecting a diffuse reflection of the optical signal from the target rather than using another cooperative target, as is shown in Fig. 1(a). The laser emits a short duration pulse which is reflected by the target; the signal is then received by the photodetector in the laser receiving system. The photodetector is connected to an integrating amplifier resulting in an output of the form shown in Fig. 1 (b). The target distance can be calculated based on the time interval ΔT as shown in Eq. (1):

$$L = \frac{c \cdot \Delta T}{2} \quad (1)$$

where L refers to the distance between the laser ranging system and the target, c is the speed of light in air and ΔT is the time interval between the laser emission and the arrival of the echo signal.

B. Laser Ranging Performance Equation

The performance of a laser ranging system is related to the laser output power, atmospheric transmission characteristics, optical system performance, and target reflection characteristics.

Eq. (2) presents an expression for the total laser power reaching the target (P_T), where the atmospheric transmission attenuation coefficient is σ , the optical unit light transmittance is T_E , and the laser output power is P_L .

$$P_T = P_L T_E e^{-L\sigma} \quad (2)$$

However, the image of the laser spot on the target may not be completely within the field of view of the receiving system due to the differences between the areas of the measured object A_{T_target} and the laser spot A_{T_spot} . Therefore, two cases should be taken into consideration during the calculation.

$$(1) A_{T_target} \geq A_{T_spot}$$

In this condition, the entire laser spot is imaged in the field of view. Eq. (3) and (4) express the target surface reflectivity R and the laser power reaching the photoelectric sensor P_R , respectively.

$$R = \frac{\rho P_T}{\pi A_T} \quad (3)$$

$$P_R = R A_T \cos(\beta + \delta) \Omega_R T_R T_f e^{-2r\sigma} \quad (4)$$

where ρ is the target reflectivity, T_R is the optical transmission ratio through the optical receiving system, T_f is the optical transmission of the narrowband filter, β is the angle between the normal of the target reflecting surface and the optical axis. Combining Eq. (3) and (4) gives a concise expression for P_R .

$$P_R = \frac{\rho P_T T_R T_f A_R \cos(\beta + \delta) \cos^3 \delta}{\pi L^2} \quad (5)$$

where A_R is the receiving lens area.

$$(2) A_{T_target} < A_{T_spot}$$

This condition indicates that the entire laser spot is not imaged in the field of view. In this case, two parameters are required to characterize the target area and the laser spot imaging ratio factor, denoted by ε and γ , respectively:

$$\varepsilon = \begin{cases} \frac{A_m}{\Omega_l L^2}, & A_m < \Omega_l L^2 \\ 1, & A_m \geq \Omega_l L^2 \end{cases}, \gamma = \begin{cases} \frac{\Omega_R}{\Omega_l}, & \Omega_R < \Omega_l \\ 1, & \Omega_R \geq \Omega_l \end{cases} \quad (6)$$

where A_m is the effective launch cross-sectional area of the target and Ω_l is the field of view of the receiving optical system.

Using Eq. (5) and (6), P_R can be represented as:

$$P_R = \frac{\gamma \varepsilon \rho P_T T_E T_R T_f A_R \cos \beta}{\pi L^2} e^{-2L\sigma} \quad (7)$$

where T_E is the transmission through the optical system used to launch the optical pulses. From Eq. (7), it can be seen that as the distance L increases, P_R decreases rapidly. When P_R decreases to the minimum detectable optical power P_{Rmin} , the corresponding distance represents the maximum range of the system L_{max} .

C. System Setup and I²C Communication

The laser ranging system comprises a laser ranging module VL53L0X, STM32F407 development board, an LCD display and a keypad to enable reset, entering the measurement and switching mode. The hardware is shown in Fig. 2(a). The VL53L0X communicates externally via the I²C interface using two bidirectional I/O signal lines: a serial data

line (SDA) and a serial clock line (SCL). The interface circuit is an open-drain output, connected to the power supply V_{CC} via a pull-up resistor. Fig. 2(b) and (c) illustrate the writing and reading transmission sequence of the I²C communication port in the VL53L0X.

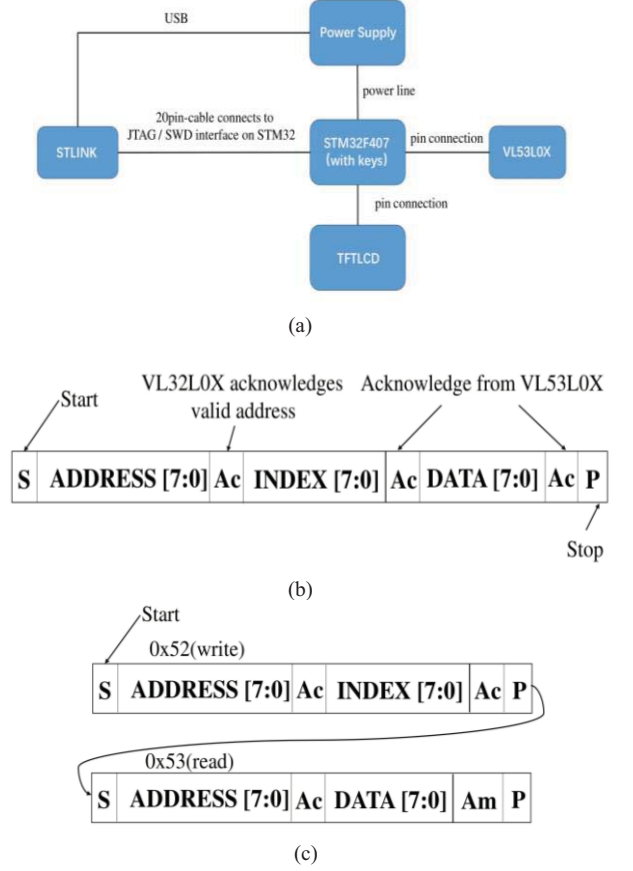


Fig. 2. (a) System setup and connections, (b) writing, and (c) reading transmission sequence of I²C communication port in the VL53L0X module.

The VL53L0X module confirms that it has received a valid address by driving down the SDA line.

In the writing sequence, the second byte received provides an 8-bit index pointing to an internal 8-bit register. After being received by the slave, the data is written into the serial/parallel registers bit by bit. An acknowledgement should follow each byte during the transmission. The data should be stored in the current index addressing internal register, when all of the data has been transmitted to the slave.

During the reading process, the contents of the register addressed by the current index are read by the consecutive address byte first. The register contents are then loaded into the serial parallel register in parallel and transmitted at the falling edge of the SCL.

D. High Accuracy Mode & Long-Distance Mode Setup

The accuracy and maximum detected range of VL53L0X are determined by the minimum detected signal intensity, sampling time period, VCSEL period and period range, etc. Therefore, two modes can be achieved by setting different values of these parameters. Timing and range are inversely proportional as shown in Eq. (8):

$$2 \cdot \text{timing} \propto \frac{1}{\sqrt{2} \cdot \text{range}} \quad (8)$$

This explains why the measured range under high accuracy mode is shorter than that of the long-range mode.

III. EXPERIMENTAL VERIFICATION

After completing the software and hardware design, trial experiments to test the system were undertaken. Expected optimization to improve the system performance would be required after preliminary verification.

A. Experiment Procedure

For the test, the target distance was first measured and marked using a tape measure. 12 distance points were selected for both modes during verification. 10 of these were from 20cm to 200 cm, with a step increase of 20 cm in each successive measurement. A further two positions at 130 cm and 210 cm were set to measure distances close to the setting range. When the measurement points had been set, the laser ranging system was placed at the marked points to carry out measurement by laser. After the experiments, the results were compared. Figure 3 shows the laser range system and the tape measure used for verification.



Fig. 3. Laser ranging system and tape measure verification equipment

B. Data Analysis

Table 1 displays the results of distances obtained using the tape measure and using the laser ranging system in the preliminary test. Here two measurement modes are applied. One is the high accuracy mode and the other is the long-distance mode. In the high accuracy mode, the maximum range which can be detected is around 120 cm, while for the long-distance mode it is around 200 cm, matching ranges defined in the code. From the data, it can be seen that when the distance exceeds the maximum detectable range in both accuracy modes, the LCD will display a fixed large constant “819.0 cm” to remind the user that the measurement is out of range. This over range warning information is defined in the VL53L0X API function rather than using text error message.

TABLE I. PRELIMINARY TEST RESULTS for TWO MODES

Real Distance(cm)	20	40	60	80	100	120
High Accuracy (cm)	22.5	43.6	63.2	82.5	102.2	125.8
Long Distance (cm)	23.6	44.3	63.8	85.6	96.4	114.8
Real distance (cm)	130	140	160	180	200	210
High Accuracy (cm)	819.0	819.0	819.0	819.0	819.0	819.0
Long Distance (cm)	125.5	135.3	165.1	187.9	203.8	819.0

In the verification, the relative accuracy is regarded as the precision standard for the laser ranging system. This parameter can be calculated using Eq. (9). The calculated accuracy results of both modes are shown in Table 2.

TABLE II. PRELIMINARY TEST RESULTS ACCURACY for TWO MODES

Real Distance (cm)	20	40	60	80	100	120
High Accuracy Error (%)	12.50	9.00	5.33	3.13	2.20	4.83
Long-distance Error (%)	18.00	10.75	6.33	7.00	3.60	4.33
Real Distance (cm)	130	140	160	180	200	210
High Accuracy Error (%)	/	/	/	/	/	/
Long-distance error (%)	3.46	3.36	3.12	4.39	1.90	/

According to the table, the measured value is close to the real value in both modes, which means the system performs satisfactorily. Typically, the error is lower as the detected distance becomes larger, while, when the value is close to maximum, the error will increase a little. In addition, the error under the high accuracy mode is always lower than that of the long-distance mode for the same distance measurement, which is expected from the software design.

$$\text{relative error} = \frac{|\text{measured value} - \text{real value}|}{\text{real value}} \times 100\% \quad (9)$$

However, for both modes, the relative error is rather high: more than 50% of the detected points have an error >5%, which means optimization is required to achieve a higher accuracy.

C. Optimization Processes and Data Analysis

In this section, the system will be optimized in two aspects: instrument improvement and code modification.

(1) Instrument Optimization

Systematic errors are among the most common errors in measuring devices, which means a relatively large error may due to systematic inaccuracies in the measurement. Here the accuracy of the tape measure used is 1 mm, therefore during optimization a vernier caliper, being a more accurate instrument, was used to reduce this error.

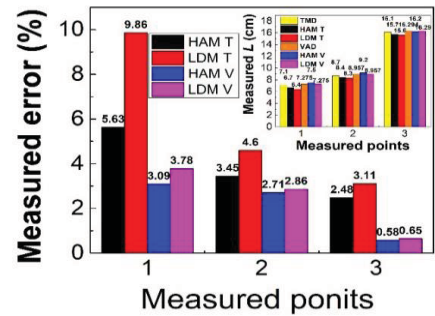


Fig.4 Measured results and accuracy for tape measure and vernier caliper

During the experiment, only three distance points within 20 cm were selected because the maximum measuring range of the vernier caliper is 20 cm. Three regular boxes were used to carry out verification of the optimization. The widths of the boxes were measured first by the tape measure and the vernier caliper, respectively, then by the laser ranging system. All the processes were the same as the preliminary test. Fig. 4 shows comparisons between the tape and vernier caliper in terms of the measurements and relative error. HAM and LDM

represent high accuracy mode and long-distance mode respectively, while T and V represent the tape measure and vernier caliper respectively. TMD and VAD mean tape measured distance and vernier caliper distance respectively.

From Fig. 4, it can be concluded that, with more precise instruments, the error between the real distance and the measured value became smaller in all experiments: when using tape measure, the error for small distances (<16 cm) can reach approximately 10% in the long-distance mode. However, when compared against measurements using the vernier caliper, the relative errors in both modes are less than 4%. This improvement becomes more obvious as the detected distance became larger, e.g. at distances around 16 cm, the error is less than 1%, representing a reduction of 1.9% and 2.46% for the high accuracy and long-distance modes, respectively. This verifies the assumption that the error may be attributed to the system error, because the accuracy level of the tape is less than that of the vernier caliper and that of the laser ranging system.

(2) Code Optimization

To improve the accuracy, the code was also modified. "vl53l0x_reset(dev)" was added into vl53l0x_gen.c file, with the purpose of reducing the error caused by switching measurement modes frequently. This is because in the preliminary test the process was simplified, simultaneous measurements of the two modes were taken at one point, then the next. Although this modification is not needed if all the distances are detected first under one mode and then switched to the other mode, in order to make the system more practical for real life applications, this optimization is necessary.

A controlled experiment was used to enable a clear comparison, meaning all the distance points, experimental processes and instruments were the same as the primary test except the code differences. The test results and the accuracy of the optimized code is shown in Fig. 5.

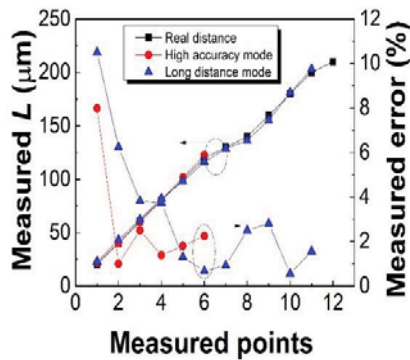


Fig. 5. Optimized code test results and accuracy for the two modes

It can be seen the accuracy of the system has been improved significantly in both the high accuracy and long-distance mode: all the measurements now have a relative error < 11%. For the high accuracy mode, when $L > 40$ cm, the error is reduced to around 1% to 2%, which is acceptable for practical applications. For the long-distance mode, the improvement is more obvious, especially at shorter distances: for 20 cm, the error is reduced by 7.5% after the code optimization. As the target distance becomes larger, the relative error is smaller, and is below 5% when the distance is >40 cm. The results indicate that for over 80% of the range of target distances, the relative error is < 5%, which means the code optimization works as expected.

(3) Optimization Combination

In the final stage, an experiment combining the two optimizations was undertaken to determine the accuracy of the improved system.

The process was similar to the instrument optimization except the code was modified. Fig. 6 shows the final results and accuracy of the system. It can be seen all the measured values have errors of around 1% -2%, satisfying the requirements of practice applications.

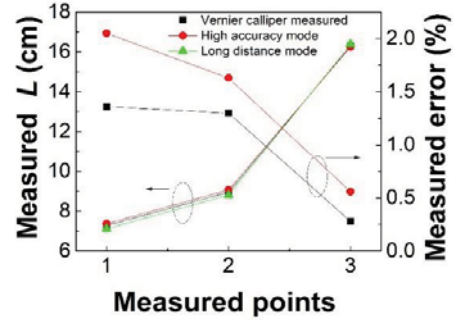


Fig. 6. Final optimized results and accuracy for two measured modes

IV. CONCLUSION

In this paper, a laser ranging system based on an STM32 processor is proposed. After inputting distance information from a laser ranging module, the measurements are displayed on an LCD display screen. The system provides two modes of measurement, with different ranges and accuracy levels: the high accuracy mode can be used for distances shorter than 120 cm while the long-distance mode can be used up to 200 cm. The error between the real distance and the value measured by the optimized laser ranging system is around 1% - 2% after using vernier caliper calibration and software optimization. There is negligible measurement fluctuations and accuracy deterioration during mode switching. Compared with traditional ranging methods, this system provides high accuracy and efficiency, satisfying the practical utilization demands, such as reversing radar for vehicles.

V. REFERENCES

- [1] Z. Wang, S. Zhu, W. Zhuo, and L. Zhu, "An Intelligent Robot based on Sound Source Location and Ultrasound Distance Detection," *Techniques of Automation & Applications*, vol. 27, pp.22-28, 2008.
- [2] Z. Diggins, N. Mahadevan, D. Herbison, E. Barth, and A. Witulski, "Impact of gamma radiation on range finding sensor performance," in *SENSORS*, 2013 IEEE, 2013: IEEE, pp. 1-4 .
- [3] B. Chen, H. Zhang, and Q. Sun, "Collimating optical systems of the pulse semiconductor laser [J]," *Laser Technology*, vol. 27, no. 3, pp. 243-244, 2003.
- [4] Y.-y. PAN, R.-z. CUI, G. CHEN, M.-I. GONG, and L. HUANG, "Beam-shaping technique for laser diode bars with prism group [J]," *Laser Technology*, vol. 30, no. 4, pp. 371-372, 2006.
- [5] Y. Hai et al., "Optical system design for small size laser ranging," in *2015 International Conference on Optoelectronics and Microelectronics (ICOM)*, 2015: IEEE, pp. 115-118.
- [6] Y. Zhao, D. Fan, M. Cao, and L. Wang, "Correction Methods of Near-Zero Step Error in Phase Laser Ranging," in *2009 Second International Workshop on Computer Science and Engineering*, 2009, vol. 2: IEEE, pp. 586-590.
- [7] S. V. F. Barreto, R. E. Sant'Anna, and M. A. F. Feitosa, "A method for image processing and distance measuring based on laser distance triangulation," in *2013 IEEE 20th International Conference on Electronics, Circuits, and Systems (ICECS)*, 2013: IEEE, pp. 695-698.
- [8] J. Liu, Y. Zhang, H. Yan, and Z. Zuo, "Proficient in STM32F4 (register version)," 2nd edition: Beijing: Beijing University of Aeronautics and Astronautics Press, 2019